Applied Surface Science 300 (2014) 8–15

Contents lists available at ScienceDirect

Applied Surface Science

journal homepage: www.elsevier.com/locate/apsusc

Surface modification of polypropylene nonwoven fabrics via covalent immobilization of nonionic sugar-based surfactants

Zhirong Xin*, Shunjie Yan, Jiaotong Ding, Zongfeng Yang, Binbin Du, Shanshan Du

School of Chemistry and Chemical Engineering, Yantai University, Yantai 264005, PR China

ARTICLE INFO

Article history:
Received 25 June 2013
Received in revised form 23 January 2014
Accepted 24 January 2014
Available online 2 February 2014

Keywords:
Polypropylene nonwoven fabrics (PP_{NWF})
Sugar-based surfactant
Photografting polymerization
Amphiphilicity
Hemocompatibility

ABSTRACT

Amphiphilic N-alkyl-1-amino-1-deoxy-*D*-glucitol (C_nAG, $n=8$, 12) were successfully prepared. Polypropylene nonwoven fabrics (PP_{NWF}) were grafted with glycidyl methacrylate (GMA) via a technique of UV-induced graft polymerization combined with plasma pre-treatment, and then PP_{NWF}-g-GMA was used for the covalent immobilization of C_nAG. The surface graft polymerization was confirmed by ATR-FTIR and XPS, respectively. Effect of grafting parameters, e.g., acetone content, monomer concentration and UV irradiation time on the grafting density of GMA was investigated. And the hemocompatibility of the modified PP_{NWF} was evaluated by protein adsorption and platelet adhesion. It was founded that the C_nAG-modified substrates greatly suppressed protein adsorption and platelet adhesion compared with the native and pGMA-grafted PP_{NWF}.

1. Introduction

Polypropylene non-woven fabrics (PP_{NWF}) have found great utility in diverse applications, due to their random network of the overlapped fibers, multiple connected pores, high thermal and chemical stability and low cost [1–3]. Despite PP_{NWF} exhibit the high potentials for comprehensive biomedical applications, there are several barriers to be overcome. Their nature hydrophobicity generally results in the activation of the coagulation factors and subsequent thrombus formation, when exposed in a physiological culture [4]. During the above procedures, the surface, which firstly interacts with proteins, platelets and cells, plays a more important role than the underlying substrate in the outer environment [5]. Thus, the control of chemistry at polymer surfaces via the modification methods has been a key issue for obtaining a desirable biocompatibility. Generally, the ever-reported modification methods can be divided into bulk and surface modification strategies. As for the bulk methods, melt grafting based on free radical polymerization is particularly attractive because of its simplicity and low cost. However, surface performances can usually not meet the requirement probably arising from the common low grafting degree of melt grafting approach. For increasing grafting degree, various methods have been proposed [6]. For example, Luan et al. developed a novel N-vinyl pyrrolidone (NVP)-assisted melt grafting method, and proposed its grafting mechanism, which will greatly promote the further development of melt grafting method [7]. They found the grafting degree of poly(ethylene glycol) methyl ether methacrylate (PEGM) monomer was increased by at least 4-fold in the presence of NVP. In addition, side reactions such as homopolyerization of the PEGM monomer were greatly reduced. More importantly, both the hydrophilicity and hemocompatibility of the graft polymer were significantly improved. In the case of the surface methods, various techniques, such as plasma treatment [8–10], ozone treatment [11], and photografting polymerization [12], were generally used for enhancing biocompatibility or antifouling properties. Among these, photo-grafting polymerization has received increasingly attention for its fast reaction rate, easy operation, simple equipment and improvement of surface properties without deteriorating the bulk performance of a material [13,14]. In addition, it enables a versatile route to multidimensionality in two and three dimensions independent of monomer types. Substances widely used in the surface modification varied from neutral materials, such as poly(ethylene glycol) (or poly(ethylene oxide)) [8,15–17], poly(N-vinyl pyrrolidone) [18–20], glycopolymers [21–26], to charged materials including heparin [27,28], chitosan [29,30], hyaluronic acid (HA) [31,32], and zwitterionic materials [33–37].

Protein adsorption is the initial event in a bio-fouling process, a reduction in protein adsorption is beneficial to the biocompatibility of a surface [38]. Note that proteins are inherently amphipathic, and therefore they can bind to hydrophobic surfaces and even hydrophilic substrates by different attachment mechanisms. A surface with solely hydrophobic or hydrophilic properties is often inadequate in resisting fouling upon the prolonged exposure to

* Corresponding author. Tel.: +86 05356902063.
E-mail address: xinzhirong2012@126.com (Z. Xin).

0169-4332/$ – see front matter © 2014 Published by Elsevier B.V.
http://dx.doi.org/10.1016/j.apsusc.2014.01.142

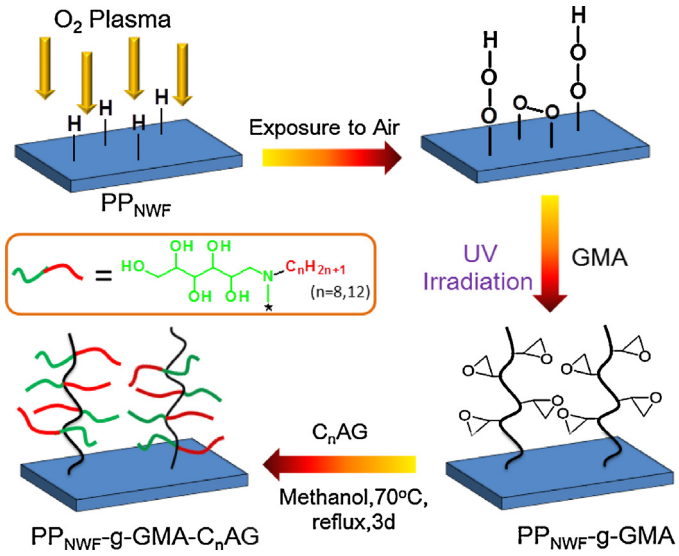

Scheme 1. Schematics of the PP_{NWF} surface modified with amphiphilic C_nAG.

complex environments [39]. Based on the above considerations, amphiphilic polymer brushes have been developed to effectively suppress nonspecific protein adsorption [35,40,41]. The adherence of proteins to amphiphilic polymer-functionalized surface via either hydrophobic or hydrophilic interactions becomes energetically unfavorable, thereby weakening the interactions of the organism with the surface. Goli et al. [42] synthesized amphiphilic brushes based on poly(2-hydroxyethyl methacrylate) (PHEMA) polymer and fluorinating moieties of different chain lengths. As for their marine antifouling properties, the fluorinated PHEMA amphiphilic layers were much better than "bare" PHEMA brushes. Chen and co-workers [43] immobilized amphiphilic homopolymer films onto substrates to study the interactions of these polymers with proteins, and found that homopolymers containing a hydrophilic and a hydrophobic functionality in every repeat unit, exhibited the reduced nonspecific protein adsorption. The similar strategy was employed by Bhatt [44] et al. and Li et al. [45] in preparing anti-biofouling surfaces based on amphiphilic polymer films.

Sugar-based surfactants refer to a kind of amphiphilic materials containing sugar moieties. The incorporation of such natural saccharide into the amphiphile structure produced interesting physicochemical and biological functionality. Much research has been focused on the hydrophilic sugar-containing polymers for the development of interfacial properties to meet the requirements of biomedical appilcations [21–26]. Up to now, there are few reports on a surface covalently modified with amphiphlic small molecular substance containing hydrophilic glucitol group and short alkyl side chains periodically for obtained biocompatibility.

The aim of this work is to investigate the biocompatible property of PP_{NWF} membranes modified by amphiphlic polymer brushes consisting of sugar-based surfactants. A series of nonionic sugar-based surfactants C_nAG with glucitol as hydrophilic groups and alkyl tails as hydrophobic group were synthesized. After the PP_{NWF} membranes were grafted with epoxy-group containing monomers, glycidyl methacrylate (GMA), via O_2 plasma pre-treatment and UV-induced graft technique, the as-prepared C_nAG were covalently immobilized on the pGMA-modified substrates based on the ring-opening of the epoxy groups (Scheme 1). The biological performances of the modified membranes, including the static protein adsorption and the platelet adhesion were investigated.

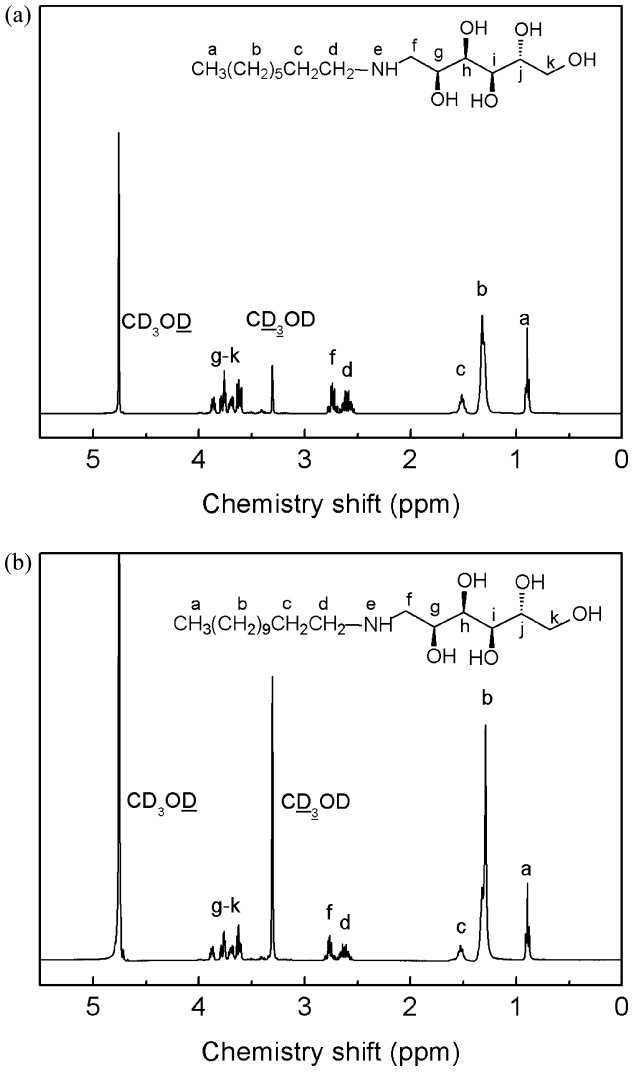

Fig. 1. ^1H NMR spectroscopy of C_8AG (a), and $C_{12}AG$ (b).

2. Materials and methods

2.1. Materials

Polypropylene nonwoven fabrics (PP_{NWF}) with an average pore diameter of 0.22 μm were purchased from Beijing

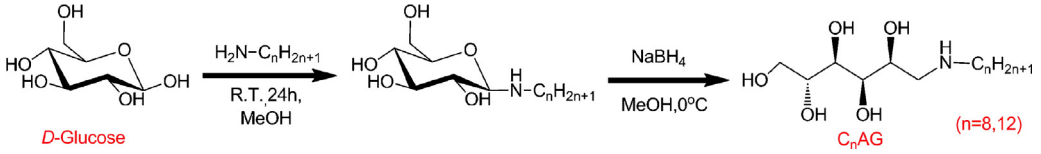

Scheme 2. Synthetic route of N-alkyl-1-deoxy-D-glucitol sugar-based surfactants.

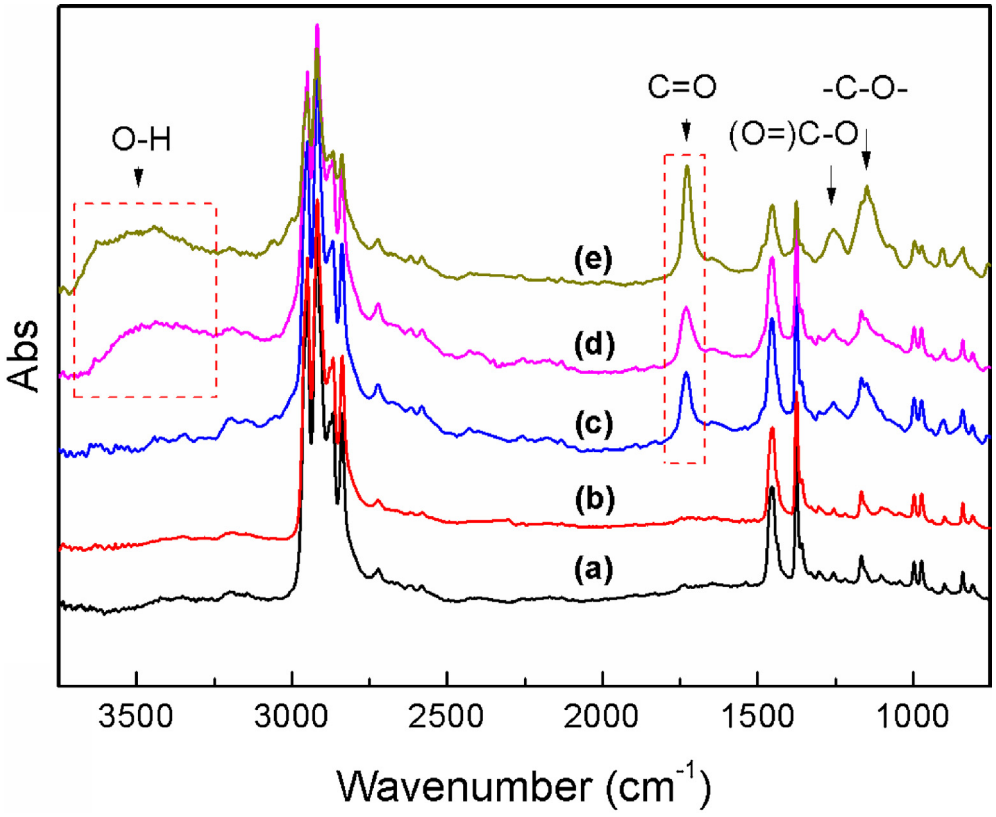

Fig. 2. ATR-FTIR spectra of the PP_{NWF} membranes. (a) The virgin membrane, (b) the plasma-treated membrane, (c) PP_{NWF}-g-GMA, (d) PP_{NWF}-g-GMA-C_8AG and (e) PP_{NWF}-g-GMA-C_{12}AG.

JDKR Co. Ltd. D-Glucose, *n*-Octylamine, and *n*-Dodecylamine were provided by Shanghai Aladdin Chemicals (China). $NaBH_4$ was supplied by Shanghai Zhanyun Chemicals (China). GMA was purchased from Aldrich and used without further pretreatment. Bovine serum albumin (BSA), sodium dodecyl sulfate (SDS) and phosphate buffered solution (PBS, 0.1 mol/L, pH = 7.4) were provided by Dingguo Bio-technology (China). Micro BCA™ protein assay reagent kits were purchased from Boster Biological Technology (AR1110, China). Other reagents were AR grade chemicals and used without further purification.

2.2. Preparation and characterization of *N-alkyl-1-amino-1-deoxy-D-glucitol surfactants*

The synthesis of N-alkyl-1-amino-1-deoxy-D-glucitol (C_nAG, n = 8, 12) (Scheme 2) used in this study has been described elsewhere [46]. Firstly, a solution of D-glucose and the proper *n*-alkylamine (*n*-Octylamine and *n*-Dodecylamine) in methanol was stirred at room temperature for 24 h. The reaction mixture was cooled to 0 °C, and a small molar excess of $NaBH_4$ was added stepwise. After that, concentrated hydrochloric acid was added drop-wise to a pH of 2–3; then the product of its hydrochloride salt form was attained. The salt was stirred with methanol and a slight molar excess of sodium methylate at room temperature for 1 d, subsequently the reaction mixture was heated under reflux. After cooling, the white precipitate was isolated, washed and dried. The structures of C_nAG were verified by proton nuclear magnetic resonance spectroscopy (^{1}H NMR, 400 MHz Bruker Avance DPX-300 spectrometer).

2.3. Surface modification of PP_{NWF} membranes

2.3.1. Preparation of the pGMA-modified membranes

The PP_{NWF} membranes were pretreated with acetone to remove residual solvent, and dried to constant weight. The dried membranes were subjected to oxygen plasma discharge by a DT-3 plasma apparatus (Suzhou Omega Technology, China) with a plasma power of 120 W for 100 s. The membranes were then immersed into the acetone/ethanol mixed solvent of GMA, and degassed for 15 min. Subsequently, graft polymerization on the PP_{NWF} was carried out under a UV light (high-pressure mercury lamp, 400 W, main wavelength 380 nm). The modified membranes (denoted as PP_{NWF}-g-GMA) were washed with deionized water and alcohol to remove the residual monomers prior to drying in a vacuum oven. Grafting density of pGMA (GD, μg/cm^2) was calculated according to the method described in the literature [17].

2.3.2. Preparation of the C_nAG-modified membranes

The PP_{NWF}-g-GMA membranes were immersed into the C_nAG methanol solution at a concentration of 50 mg/mL. Then the mixture was stirred at 70 °C for 72 h under reflux. After that, the membranes were soaked in stirring distilled water and ethanol alternately at 60 °C for 24 h, and dried under vacuum to obtain the C_nAG-modified membranes (denoted as PP_{NWF}-g-GMA-C_nAG). Grafting density (GD, μg/cm^2) of C_nAG was also calculated as previously [18].

2.4. Characterization of surface chemistry

ATR-FTIR spectra of the membranes were obtained from a Fourier transform infrared spectrometer (FTIR, BRUKER Vertex 70) with a resolution of 4 cm^{-1} in absorbance mode.

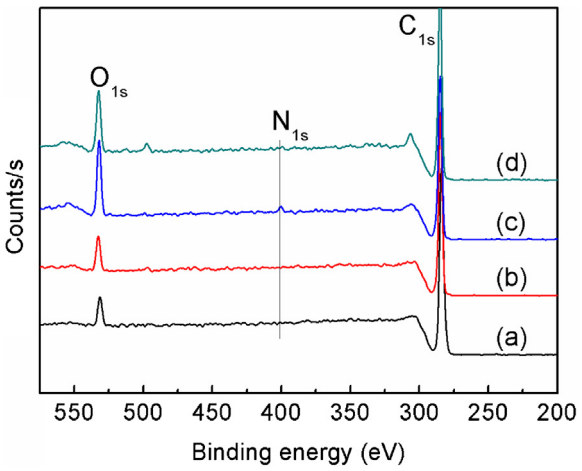

Fig. 3. XPS spectra of the PP_{NWF} membranes. (a) The virgin membrane, (b) PP_{NWF}-g-GMA, (c) PP_{NWF}-g-GMA-C_8AG, and (d) PP_{NWF}-g-GMA-C_{12}AG.

X-ray photoelectron spectroscopy was obtained on a VG Scientific ESCA MK II Thermo Avantage V 3.20 analyzer with an Al/K ($h\nu$ = 1486.6 eV) anode mono-X-ray source. The releasing angle of the photoelectron for each atom was fixed at 90°. The spectra were collected over a range of 0–1200 eV and the C_{1s} peak was resolved by computer simulation into its constituent peaks.

2.5. Protein adsorption

The membranes were placed in individual wells of a 24 well tissue culture plate, and PBS solution was added. After the equilibration at 37 °C for at least 12 h, the membranes were incubated in protein solution of BSA at a concentration of 1.0 mg/mL at 37 °C for 2 h. After incubation, the samples carefully rinsed with PBS were immersed in an aqueous solution of 1.0 wt% SDS and subjected to ultrasonic treatment for 60 min to remove the proteins adsorbed on the surfaces. Based on the bicinchoninic acid (BCA) protein assay kit method, the protein concentration in the SDS solution was determined by a TECAN SUNRISE microplate reader. The amount of proteins adsorbed on the surfaces was calculated.

2.6. Platelet adhesion

Firstly, the membranes were incubated in a tissue culture plate with PBS for 2 h. Then 20 μL of fresh platelet-rich plasma obtained from the fresh rabbit by centrifugation at 1000 rpm for 15 min was dropped on each membrane and incubated at 37 °C for 60 min. After washing with PBS, the adhered platelets on the membranes were fixed by 2.5 wt% glutaraldehyde for more than 10 h at 4 °C. Finally, the membranes were washed with PBS several times and dehydrated with a series of ethanol/water mixtures (30, 50, 70, 90, 100 vol% ethanol) for half an hour in each step. The samples were observed with a field emitted scanning electron microscopy (SEM, XL 30 ESEM FEG, FEI Company, USA).

3. Results and discussion

3.1. Preparation of N-alkyl-1-amino-1-deoxy-D-glucitols (C_nAG)

Nonionic C_nAGs with different hydrocarbon tails were prepared from the easily accessible, inexpensive and renewable D-glucose and *n*-alkylamines. The key feature of C_nAG is the covalent coupling of a hydrophilic saccharide group with a lipophilic alkyl chain through a nitrogen (amine) linkage [46]. Actually, amphiphilic C_nAG are often used as nonionic sugar-based surfactants when the hydrocarbon tail length is equal or greater than 8 carbons.

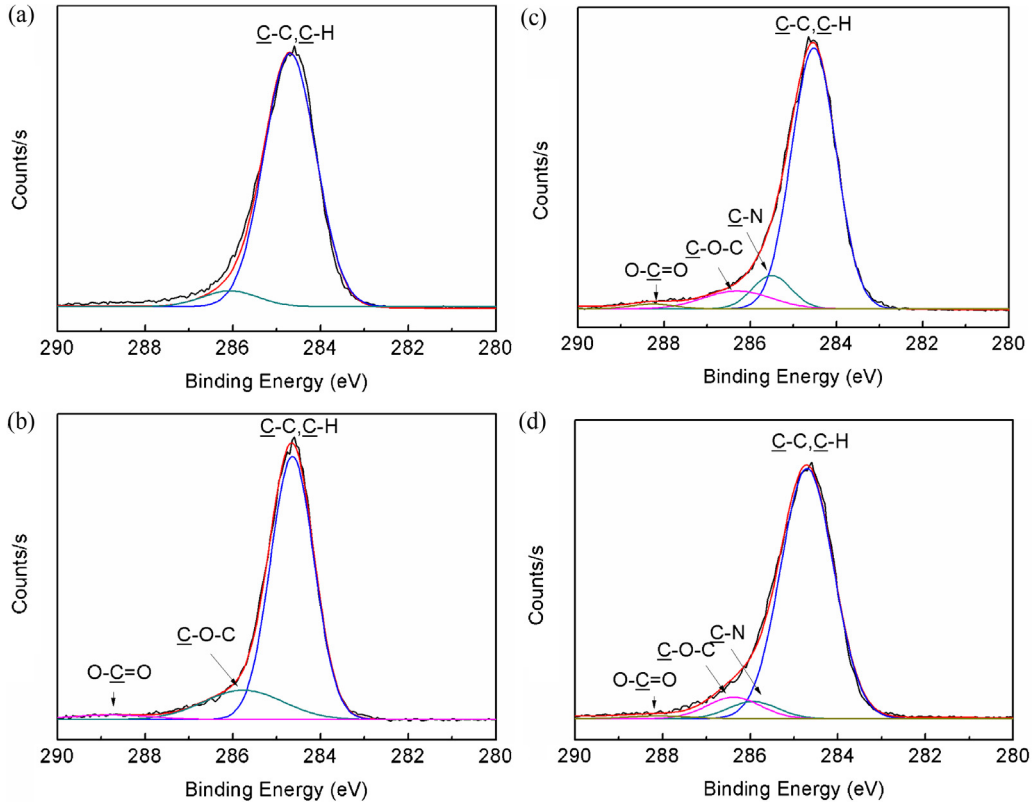

Fig. 4. High-resolution C_{1s} spectra and their fitting curves. (a) The virgin membrane, (b) PP_{NWF}-g-GMA, (c) PP_{NWF}-g-GMA-C_8AG and (d) PP_{NWF}-g-GMA-C_{12}AG.

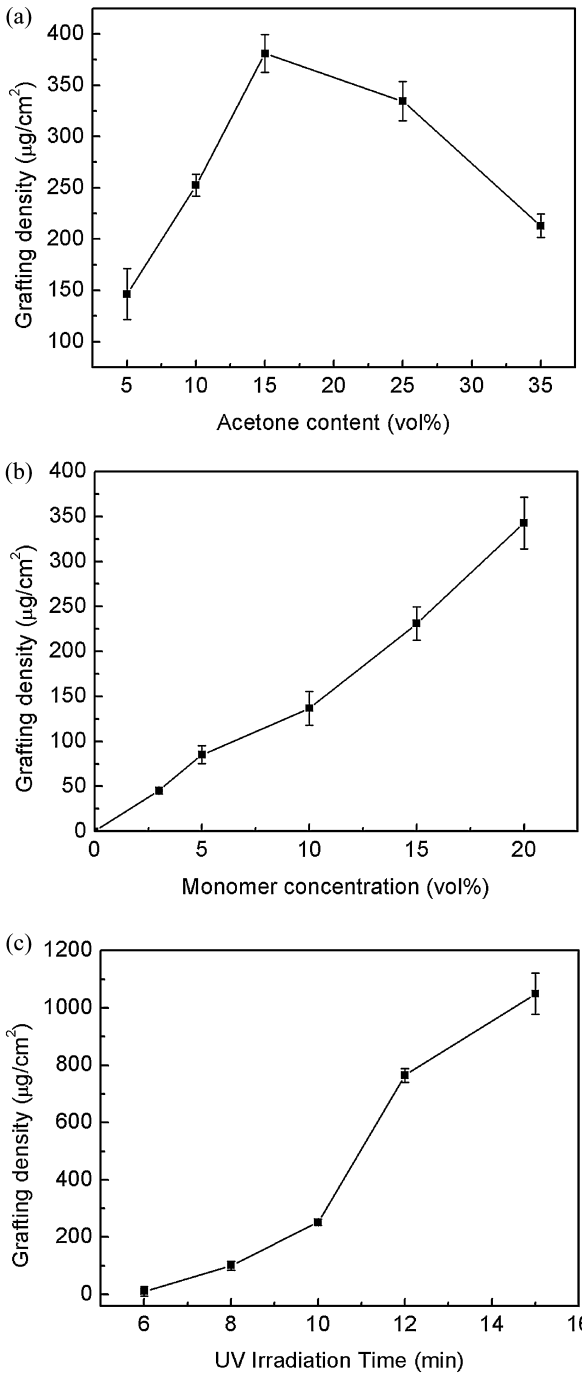

Fig. 5. Grafting density of pGMA on the PP_{NWF} membranes versus acetone content (UV irradiation time: 8 min, GMA concentration: 10 vol%) (a), GMA concentration (acetone content: 10 vol%, UV irradiation time: 8 min) (b), and UV irradiation time (acetone content: 10 vol%, GMA concentration: 10 vol%) (c).

The ^{1}H NMR spectra of the C_nAG were shown in Fig. 1(a, b), and the corresponding proton chemical shifts were summarized as follows.

N-octyl-1-amino-1-deoxy-D-glucitol, C_8AG, (CD_3OD): (δ, ppm) 0.89 (t, 3H, $C\underline{H}_3$); 1.32 (m, 10H, $CH_3(C\underline{H}_2)_5$); 1.55 (m, 2H, N-$CH_2C\underline{H}_2(CH_2)_5$); 2.54–2.78 (m, 4H, N-$C\underline{H}_2$); 3.56–3.88 (m, 6H, $C\underline{H}$-OH and–$\underline{CH}_2$-OH, sugar).

N-dodecyl-1-amino-1-deoxy-D-glucitol, C_{12}AG, (CD_3OD): (δ, ppm) 0.90 (t, 3H, $C\underline{H}_3$); 1.29 (m, 18H, $CH_3(C\underline{H}_2)_9$); 1.53 (m, 2H, N-$CH_2C\underline{H}_2(CH_2)_9$); 2.59–2.76 (m, 4H, N-$C\underline{H}_2$); 3.59–3.88 (m, 6H, $C\underline{H}$-OH and–$\underline{CH}_2$-OH, sugar).

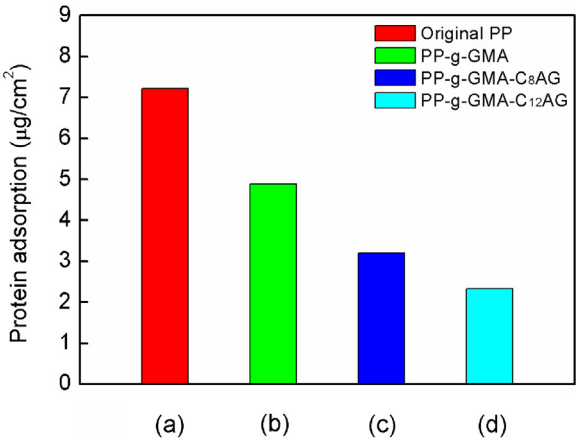

Fig. 6. Protein adsorption on the PP_{NWF} membranes (The membranes with grafting density (μg/cm^2) of 347 (b), 660 (c), and 723 (d)).

All of the above data were in good agreement with the proposed structures, which confirmed that nonionic sugar-based surfactants were obtained.

3.2. Surface modification of the PP_{NWF} membranes

3.2.1. Surface chemistry

After the membranes were subjected to the experiments as shown in Scheme 1, the surface chemical feature of the PP_{NWF} membranes was examined by ATR-FTIR (Fig. 2). As reported, although plasma treatment introduced various polar groups, e.g., peroxide, hydroxyl group and carboxyl group [5], the layer was too thin to be detected, thus there was no obvious difference between the virgin and plasma-treated membranes in the spectra (Fig. 2(a, b)). In the FTIR curve of the pGMA-modified membrane (Fig. 2(c)), the new peaks at about 1660 and 1150 cm^{-1} corresponding to the absorption of carbonyl group and the stretching vibration of C—O bond were respectively observed. It suggested that pGMA was successfully grafted onto the PP_{NWF} substrates. After the further immobilization of C_nAG onto the pGMA-grafted membrane (Fig. 2(d, e)), the existence of some peaks including the peak at 1660 cm^{-1} (C═O stretching vibrations), the peak at 1260 and 1150 cm^{-1} (C(═O)—O and C—O stretching vibrations), and a new broad peak at 3440 cm^{-1} (stretching vibration of hydroxyl group) confirmed that the amphiphilic C_nAG were immobilized onto the PP_{NWF}-g-GMA membranes.

All membranes were further analyzed by XPS allowing for an elemental analysis of the outermost layer of the films. As evident from Fig. 3, one large peak at about 284 eV attributing to C_{1s} was found in the virgin PP_{NWF} membrane. The small peak at about 530 eV corresponding to O_{1s} was attributed to the oxygen contamination as reported by other researchers [47]. The pGMA-modified PP_{NWF} membrane showed an increased peak at 530 eV that was attributed to the GMA units. The newly appeared peak at 400 eV attributing to N_{1s} and the greatly enhanced intensity of O_{1s} peak on the modified membrane suggested the further immobilization of C_nAG onto the membrane, which also could be confirmed by the high-resolution XPS spectra and their peak fitting curves (Fig. 4). The C_{1s} high-resolution curve of virgin membrane (Fig. 4(a)) was decomposed into two peaks using a Gaussian peak fitting algorithm. The C_{1s} high-resolution spectrum of the pGMA-modified membrane was composed of three carbon components (Fig. 4(b)), i.e., $\underline{C}$—C at 284.8 eV, $\underline{C}$—O—C at 286 eV and O—$\underline{C}$═O at 288.4 eV. Correspondingly, the each spectra of PP_{NWF}-g-GMA-C_nAG (Fig. 4(c, d)) was composed into four peaks: a $\underline{C}$—C peak at 284.8 eV, a $\underline{C}$—N peak at 285.6 eV, a $\underline{C}$—O—C peak at 286.3 eV, and O—$\underline{C}$═O at 288.4 eV.

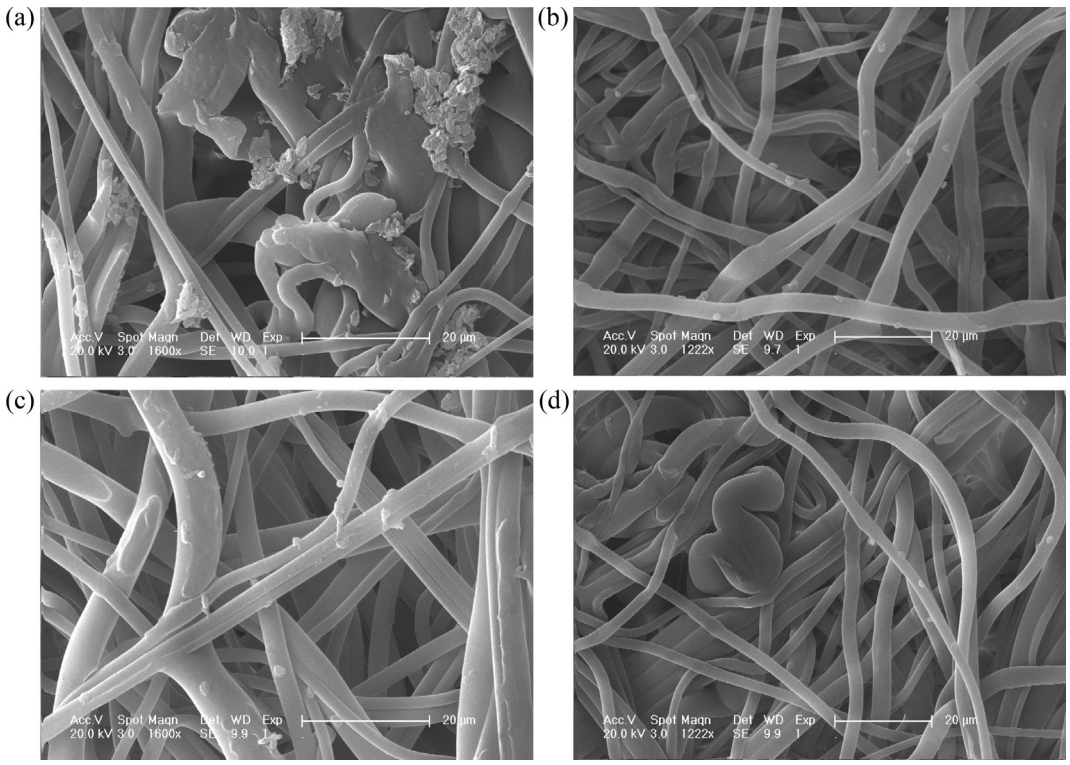

Fig. 7. SEM pictures of platelets adhesion on the PP_{NWF} membrane. (a) The virgin membrane, (b) PP_{NWF}-g-GMA, (c) PP_{NWF}-g-GMA-C_8AG and (d) PP_{NWF}-g-GMA-C_{12}AG.

According to the above XPS data, the atomic compositions and atomic ratio (N/C) on the surfaces were calculated and summarized in Table 1. After the surface modification, the atomic ratio value of N/C was decreased from 0.19 to 0.13 as the hydrocarbon tails length increased. These verified the successful surface modification of PP_{NWF} via the procedures as shown in Scheme 1.

3.2.2. *Effect of grafting parameters on the grafting density of GMA*

During the pGMA grafting polymerization process, the effect of acetone content, monomer concentration and UV irradiation time were investigated to acquire the relationship between reaction conditions and grafting density. As shown in Fig. 5(a), the grafting density of pGMA underwent an initially rapid increase, attained a maximum value at 15 vol% acetone content, and finally decreased as the acetone concentration increased. This phenomenon was due to that acetone not only promoted monomer solubility for the ease of chain growing, but also participated in the polymerization chain transfer from polymer surface to the solvent. When the two effects achieved a balance, an optimal grafting density was presented. It also could be found that grafting density increased along with monomer concentration due to the enlarged probability of effective collision between the monomers and active sites excited on the membrane surface (Fig. 5(b)). UV irradiation time had a similar effect on the grafting density to the monomer concentration (Fig. 5(c)). Increasing the irradiation time, more active sites were introduced on the substrates, thus a higher grafting density was obtained. In detail, as the UV time range from 6 to 15 min, the grafting density at UV 6 min was too low to be observed, while a very grafting density of about 1000 μg/cm^2 after 15 min was obtained, which attributed to random network of overlapped fibers and multiple connected pores of PP_{NWF}. These results confirmed that the grafting density could be adjusted by controlling the grafting parameters.

Table 1
Atomic compositions and atomic ratio (N/C) from XPS.

Samples	Atomic compositions (at.%)			Atomic ratio
	C_{1s}	N_{1s}	O_{1s}	N/C
Virgin PP_{NWF}	94.32	–	5.68	–
PP_{NWF}-g-GMA	92.22	–	7.78	–
PP_{NWF}-g-GMA-C_8AG	82.70	15.75	1.55	0.19
PP_{NWF}-g-GMA-C_{12}AG	88.32	11.06	0.62	0.13

3.3. *Protein adsorption*

Many factors affected the antifouling properties, such as surface character, surface free energy, solution environment, and the surface morphology [48]. The amount of proteins adhered on the surface is an important factor in evaluating the biocompatibility of a material. A reduction of protein adsorption can suppress platelet adhesion on the surface. Herein, BSA was selected as a model protein to assess the protein adsorption on the virgin and the modified PP_{NWF} membranes. The protein adsorption of virgin PP_{NWF} membrane, PP_{NWF}-g-GMA and PP_{NWF}-g-GMA-C_nAG were illustrated in Fig. 6. On the virgin and pGMA-modified membranes surface, the adsorption amounts were 7.2 μg/cm^2 and 4.9 μg/cm^2 at a BSA concentration of 1.0 mg/mL, respectively, which exhibited a strong interaction between proteins and the membrane surface. In contrast, the adsorption of PP_{NWF}-g-GMA-C_8AG and PP_{NWF}-g-GMA-C_{12}AG were 3.2 μg/cm^2 and 2.3 μg/cm^2, which decreased by at least 55% and 68% compared with the original membrane. Besides the amphiphilic C_nAG modified samples, we hypothesized that the alkyl chain length of the sugar-based surfactants would influence the extent of protein adsorption. We attribute this to the assumption that the hydrophilic and hydrophobic groups of C_nAG should be similar in length to achieve the optimized surface presentation, where neither hydrophilic nor hydrophobic functional groups dominate the presentation. Considering the results of protein adsorption, the C_8AG- and C_{12}AG-modified surfaces could achieve an enhanced balance of hydrophobicity and

hydrophilicity and would be able to present the desired periodic conformation for protein adsorption resistance. The proposed mechanism was that if part of the surface in the protein has an affinity for the hydrophilic domain of the amphiphilic membrane then the hydrophobic part of the polymer will be incompatible with the binding and vice versa [43]. Thus, the adherence of proteins to membrane surface via either hydrophobic or hydrophilic interactions becomes energetically unfavorable, thereby suppressing the protein adsorption.

3.4. Platelet adhesion

When contacted with a foreign surface, plasma proteins firstly adsorbed to the surface, followed by platelet adhesion and activation, coagulation, complement activation and other blood cell responses [49]. Thus, platelet adhesion on a substrate is another important tool for evaluating the biocompatibility. PP_{NWF} is nonpolar, chemically inert, and of multiple connected pores. Besides, the high interfacial free energy and porous structure promoted protein adsorption and platelet adhesion. As shown in Fig. 7(a), a large number of platelets aggregated and adhered on the virgin PP_{NWF} surface, and the deposited platelets on the surface exhibited spreading shape (activated state, late pseudopodial, hyaloplasm spreading) and fully spread shape (activated state, hyaloplasm well spread, no distinct pseudopodia) [50]. This probably because that the surface of virgin membrane possessed the largest protein adsorption amount in the above protein assay. Once the protein coats the surface, living cells will interact directly with the adsorbed proteins to translate biometrical physical and chemical properties into a "biological language" [51]. While on PP_{NWF}-g-GMA substrate (Fig. 7(b)), the amount of adhered platelets was somewhat decreased and platelet adhesion was inhibited to some extent. Interestingly, the amount of platelets on PP_{NWF}-g-GMA-C_nAG (Fig. 7(c, d)) substrates was obviously decreased and most of the platelets adhered on the membrane maintained the unactivated shape (round or discoid, no pseudopodia present). The platelet adhesion test revealed that surfaces modified by amphiphilic sugar-based surfactants showed improved biocompatibility upon direct exposure to plasma environment when compared with the virgin PP_{NWF} membrane.

4. Conclusions

Amphiphilic C_nAGs with different hydrocarbon tails have been successfully prepared by condensation of long chain amines onto saccharide and subsequent reduction of the N-alkylglucamines. The PP_{NWF} have been grafted with pGMA by means of a technique of UV-induced graft polymerization combined with oxygen plasma pre-treatment, followed by grafting of C_nAG. The chemical structures of C_nAG and relevant modification have been confirmed by ^{1}H NMR, ATR-FTIR and XPS, respectively. Effect of grafting parameters such as acetone content, monomer concentration and UV irradiation time on the grafting density of GMA of has been obtained. The C_nAG-modified substrates, which possessed a good balance of hydrophobicity and hydrophilicity, could suppress protein adsorption and platelet adhesion compared with the native and pGMA-grafted PP_{NWF}.

Acknowledgement

The authors acknowledge the financial support of the National Science Foundation of China (No. 50873084), and the Shandong Natural Science Foundation of China (Grant No. ZR2010BM029).

References

[1] J.P. Chen, C.Y. Kuo, W.L. Lee, Thermo-responsive wound dressings by grafting chitosan and poly(N-isopropylacrylamide) to plasma-induced graft polymerization modified non-woven fabrics, Appl. Surf. Sci. 262 (2012) 95–101.
[2] Y. Zheng, H. Liu, P.V. Gurgel, R.G. Carbonell, Polypropylene nonwoven fabrics with conformal grafting of poly(glycidyl methacrylate) for bioseparations, J. Membr. Sci. 364 (2010) 362–371.
[3] J. Zhao, Q. Shi, S. Luan, L. Song, H. Yang, P. Stagnaro, J. Yin, Polypropylene non-woven fabric membrane via surface modification with biomimetic phosphorylcholine in Ce(IV)/HNO_3 redox system, Mater. Sci. Eng.: C 32 (2012) 1785–1789.
[4] D. Li, H. Chen, J.L. Brash, Mimicking the fibrinolytic system on material surfaces, Colloids Surf. B: Biointerfaces 86 (2011) 1–6.
[5] K. Kato, E. Uchida, E.T. Kang, Y. Uyama, Y. Ikada, Polymer surface with graft chains, Prog. Polym. Sci. 28 (2003) 209–259.
[6] E. Passaglia, S. Coiai, S. Augier, Control of macromolecular architecture during the reactive functionalization in the melt of olefin polymers, Prog. Polym. Sci. 34 (2009) 911–947.
[7] H.W. Yang, S.F. Luan, J. Zhao, H.C. Shi, X.M. Li, L.J. Song, J. Jin, Q. Shi, J.H. Yin, D. Shi, P. Stagnaro, Improving hemocompatibility of styrene-b-(ethylene-co-butylene)-b-styrene elastomer via N-vinyl pyrrolidone-assisted grafting of poly(ethylene glycol) methacrylate, Polymer 53 (2012) 1675–1683.
[8] S. Zanini, P. Massini, M. Mietta, E. Grimoldi, C. Riccardi, Plasma treatments of PET meshes for fuel-water separation applications, J. Colloid Interface Sci. 322 (2008) 566–571.
[9] S. Zanini, C. Riccardi, M. Orlandi, C. Colombo, F. Croccolo, Plasma-induced graft-polymerisation of ethylene glycol methacrylate phosphate on polyethylene films, Polym. Degrad. Stab. 93 (2008) 1158–1163.
[10] K.M. Xiu, Q. Cai, J.S. Li, X.P. Yang, W.T. Yang, F.J. Xu, Anti-fouling surfaces by combined molecular self-assembly and surface-initiated ATRP for micropatterning active proteins, Colloids Surf. B: Biointerfaces 90 (2012) 177–183.
[11] J.M. Xu, Y.L. Yuan, B. Shan, J. Shen, S.C. Lin, Ozone-induced grafting phosphorylcholine polymer onto silicone film to improve hemocompatibility, Colloids Surf. B: Biointerfaces 35 (2004) 259.
[12] J. Deng, L. Wang, L. Liu, W. Yang, Developments and new applications of UV-induced surface graft polymerizations, Prog. Polym. Sci. 34 (2009) 156–193.
[13] U. Edlund, M. Källrot, A.C. Albertsson, Single-step covalent functionalization of polylactide surfaces, J. Am. Chem. Soc. 127 (2005) 8865–8871.
[14] M. Kallrot, U. Edlund, A.C. Albertsson, Surface functionalization of porous resorbable scaffolds by covalent grafting, Macromol. Biosci. 8 (2008) 645–654.
[15] X. Li, S. Luan, H. Yang, H. Shi, J. Zhao, J. Jin, J. Yin, P. Stagnaro, Surface modification of poly(styrene-b-(ethylene-co-butylene)-b-styrene) elastomer via photo-initiated graft polymerization of poly(ethylene glycol), Appl. Surf. Sci. 258 (2012) 2344–2349.
[16] S. Zanini, M. Orlandi, C. Colombo, E. Grimoldi, C. Riccardi, Plasma-induced graft-polymerization of polyethylene glycol acrylate on polypropylene substrates, Eur. Phys. J. D 54 (2009) 159–164.
[17] S. Zanini, M. Muller, C. Riccardi, M. Orlandi, Polyethylene glycol grafting on polypropylene membranes for anti-fouling properties, Plasma Chem. Plasma Process. 27 (2007) 446–457.
[18] S. Luan, J. Zhao, H. Yang, H. Shi, J. Jin, X. Li, J. Liu, J. Wang, J. Yin, P. Stagnaro, Surface modification of poly(styrene-b-(ethylene-co-butylene)-b-styrene) elastomer via UV-induced graft polymerization of N-vinyl pyrrolidone, Colloids Surf. B: Biointerfaces 93 (2012) 127–134.
[19] M. Källrot, U. Edlund, A.C. Albertsson, Surface functionalization of degradable polymers by covalent grafting, Biomaterials 27 (2006) 1788–1796.
[20] M. Kallrot, U. Edlund, A.C. Albertsson, Covalent grafting of poly(L-lactide) to tune the in vitro degradation rate, Biomacromolecules 8 (2007) 2492–2496.
[21] Q. Yang, M. Strathmann, A. Rumpf, G. Schaule, M. Ulbricht, Grafted glycopolymer-based receptor mimics on polymer support for selective adhesion of bacteria, ACS Appl. Mater. Interfaces 2 (2010) 3555–3562.
[22] Q. Yang, Z.K. Xu, Z.W. Dai, J.L. Wang, M. Ulbricht, Surface modification of polypropylene microporous membranes with a novel glycopolymer, Chem. Mater. 17 (2005) 3050–3058.
[23] Q. Yang, J. Tian, Z.W. Dai, M.X. Hu, Z.K. Xu, Novel photoinduced grafting-chemical reaction sequence for the construction of a glycosylation surface, Langmuir 22 (2006) 10097–10102.
[24] Q. Yang, M.X. Hu, Z.W. Dai, J. Tian, Z.K. Xu, Fabrication of glycosylated surface on polymer membrane by UV-induced graft polymerization for lectin recognition, Langmuir 22 (2006) 9345–9349.
[25] Q. Yang, Z.K. Xu, M.X. Hu, J.J. Li, J. Wu, Novel sequence for generating glycopolymer tethered on a membrane surface, Langmuir 21 (2005) 10717–10723.
[26] H.Y. Yu, M.X. Hu, Z.K. Xu, Improvement of surface properties of poly(propylene) hollow fiber microporous membranes by plasma-induced tethering of sugar moieties, Plasma Process Polym. 2 (2005) 627–632.
[27] U. Edlund, S. Danmark, A.C. Albertsson, A strategy for the covalent functionalization of resorbable polymers with heparin and osteoinductive growth factor, Biomacromolecules 9 (2008) 901–905.
[28] Y.C. Kuo, Y.T. Tsai, Heparin-conjugated scaffolds with pore structure of inverted colloidal crystals for cartilage regeneration, Colloids Surf. B: Biointerfaces 82 (2011) 616–623.
[29] O. Wiarachai, N. Thongchul, S. Kiatkamjornwong, V.P. Hoven, Surface-quaternized chitosan particles as an alternative and effective organic antibacterial material, Colloids Surf. B: Biointerfaces 92 (2012) 121–129.

[30] Y.F. Wang, Q.F. Hong, Y.J. Chen, X.X. Lian, Y.F. Xiong, Surface properties of polyurethanes modified by bioactive polysaccharide-based polyelectrolyte multilayers, Colloids Surf. B: Biointerfaces 100 (2012) 77–83.
[31] X. Li, S. Luan, H. Shi, H. Yang, L. Song, J. Jin, J. Yin, P. Stagnaro, Improved biocompatibility of poly (styrene-b-(ethylene-co-butylene)-b-styrene) elastomer by a surface graft polymerization of hyaluronic acid, Colloids Surf. B: Biointerfaces 102 (2013) 210–217.
[32] X. Li, S. Luan, S. Yuan, L. Song, J. Zhao, J. Ma, H. Shi, H. Yang, J. Jin, J. Yin, Surface functionalization of styrenic block copolymer elastomeric biomaterials with hyaluronic acid via a grafting to strategy, Colloids Surf. B: Biointerfaces 112 (2013) 146–154.
[33] J. Zhao, Q. Shi, S. Luan, L. Song, H. Yang, H. Shi, J. Jin, X. Li, J. Yin, P. Stagnaro, Improved biocompatibility and antifouling property of polypropylene nonwoven fabric membrane by surface grafting zwitterionic polymer, J. Membr. Sci. 369 (2011) 5–12.
[34] Y.F. Yang, Y. Li, Q.L. Li, L.S. Wan, Z.K. Xu, Surface hydrophilization of microporous polypropylene membrane by grafting zwitterionic polymer for anti-biofouling, J. Membr. Sci. 362 (2010) 255–264.
[35] Y. Li, C.M. Liu, J.Y. Yang, Y.H. Gao, X.S. Li, G.H. Que, J.R. Lu, Anti-biofouling properties of amphiphilic phosphorylcholine polymer films, Colloids Surf. B: Biointerfaces 85 (2011) 125–130.
[36] L. Song, J. Zhao, S. Luan, J. Ma, J. Liu, X. Xu, J. Yin, Fabrication of a detection platform with boronic-acid-containing zwitterionic polymer brush, ACS Appl. Mater. Interfaces 5 (2013) 13207–13215.
[37] B. Byambaa, T. Konno, K. Ishihara, Cell adhesion control on photoreactive phospholipid polymer surfaces, Colloids Surf. B: Biointerfaces 99 (2012) 1–6.
[38] M. Mrksich, A surface chemistry approach to studying cell adhesion, Chem. Soc. Rev. 29 (2000) 267–273.
[39] S. Colak, G.N. Tew, Amphiphilic polybetaines: the effect of side-chain hydrophobicity on protein adsorption, Biomacromolecules 13 (2012) 1233–1239.
[40] I. Banerjee, R.C. Pangule, R.S. Kane, Antifouling coatings: recent developments in the design of surfaces that prevent fouling by proteins, bacteria, and marine organisms, Adv. Mater. 23 (2011) 690–718.
[41] K.H. Hwangbo, Y.J. Kim, K.Y. Cho, Fabrication of protein-resistant blend based on PVDF-HFP and amphiphilic brush copolymer made from PMMA and PEGMA, Appl. Surf. Sci. 263 (2012) 291–296.
[42] K.K. Goli, O.J. Rojas, J. Genzer, Formation and antifouling properties of amphiphilic coatings on polypropylene fibers, Biomacromolecules 13 (2012) 3769–3779.
[43] Y. Chen, S. Thayumanavan, Amphiphilicity in homopolymer surfaces reduces nonspecific protein adsorption, Langmuir 25 (2009) 13795–13799.
[44] S. Bhatt, J. Pulpytel, G. Ceccone, P. Lisboa, F. Rossi, V. Kumar, F. Arefi-Khonsari, Nanostructure protein repellant amphiphilic copolymer coatings with optimized surface energy by inductively excited low pressure plasma, Langmuir 27 (2011) 14570–14580.
[45] J.H. Li, M.Z. Li, J. Miao, J.B. Wang, X.S. Shao, Q.Q. Zhang, Improved surface property of PVDF membrane with amphiphilic zwitterionic copolymer as membrane additive, Appl. Surf. Sci. 258 (2012) 6398–6405.
[46] U. Laska, K.A. Wilk, I. Maliszewska, L. Syper, Novel glucose-derived gemini surfactants with a 1,1′-ethylenebisurea spacer: preparation, thermotropic behavior, and biological properties, J. Surfactants Detergents 9 (2006) 115–124.
[47] V.B. Sadhu, A. Perl, M. Peter, D.I. Rozkiewicz, G. Engbers, B.J. Ravoo, D.N. Reinhoudt, J. Huskens, Surface modification of elastomeric stamps for microcontact printing of polar inks, Langmuir 23 (2007) 6850–6855.
[48] M.T. Bernards, G. Cheng, Z. Zhang, S. Chen, S. Jiang, Nonfouling polymer brushes via surface-initiated, two-component atom transfer radical polymerization, Macromolecular 41 (2008) 4216–4219.
[49] R. Jahangir, C.B.M. Closkey, W.G.M. Clung, R.S. Labow, J.L. Brash, J.P. Santerre, The influence of protein adsorption and surface modifying macromolecules on the hydrolytic degradation of a poly(ether-urethane) by cholesterol esterase, Biomaterials 24 (2003) 121–130.
[50] J.C. Lin, T.M. Ko, S.L. Cooper, Polyethylene surface sulfonation: surface characterization and platelet adhesion studies, J. Colloid Interface Sci. 164 (1994) 99–106.
[51] C.J. Wilsonl., R.E. Clegg, D.I. Leavesley, M.J. Pearcy, Mediation of biomaterial-cell interactions by adsorbed proteins: a review, Tissue Eng. 11 (2005) 1–18.